The Astrophysical Journal Letters, 918:L19 (6pp), 2021 September 1 https://doi.org/10.3847/2041-8213/ac1e2e

A Sample Bias in Quasar Variability Studies

Yue Shen[1,2] and Colin J. Burke[1,3]
[1] Department of Astronomy, University of Illinois at Urbana-Champaign, Urbana, IL 61801, USA
[2] National Center for Supercomputing Applications, University of Illinois at Urbana-Champaign, Urbana, IL 61801, USA
[3] Center for AstroPhysical Surveys, National Center for Supercomputing Applications, University of Illinois at Urbana-Champaign, Urbana, IL 61801, USA
Received 2021 July 23; revised 2021 August 6; accepted 2021 August 17; published 2021 August 31

Abstract

When a flux-limited quasar sample is observed at later times, there will be more dimmed quasars than brightened ones, due to a selection bias induced at the time of sample selection. Quasars are continuously varying and there are more fainter quasars than brighter ones. At the time of selection, even symmetrical variability will result in more quasars with their instantaneous fluxes scattered above the flux limit than those scattered below, leading to an asymmetry in flux changes over time. The same bias would lead to an asymmetry in the ensemble structure function (SF) of the sample such that the SF based on pairs with increasing fluxes will be slightly smaller than that based on pairs with decreasing fluxes. We use simulated time-symmetric quasar light curves based on the damped random walk prescription to illustrate the effects of this bias. The level of this bias depends on the sample, the threshold of magnitude changes, and the coverage of light curves, but the general behaviors are consistent. In particular, the simulations matched to recent observational studies with decade-long light curves produce an asymmetry in the SF measurements at the few percent level, similar to the observed values. These results provide a cautionary note on the reported time asymmetry in some recent quasar variability studies.

Unified Astronomy Thesaurus concepts: Quasars (1319); Surveys (1671); Black hole physics (159)

1. Introduction

Recent wide-field optical time-domain surveys have greatly improved the statistics for quasar variability studies (e.g., Vanden Berk et al. 2004; de Vries et al. 2005; Bauer et al. 2009; MacLeod et al. 2010; Caplar et al. 2017). Optical variability of quasars mostly traces the variations from the accretion disk emission, and is observed to be stochastic and ubiquitous over the full ranges of timescales and quasar properties. However, the nature of quasar variability is still largely unknown, and observations of the ensemble quasar variability properties potentially can be used to understand the origin of the optical variability of quasars. For example, Kawaguchi et al. (1998) proposed to use the structure function (SF) of quasar variability to distinguish different models, based on the asymmetry in the SF measured from brightening or fading pairs:

$$\beta(\tau) = \frac{\mathrm{SF_{ic}}(\tau) - \mathrm{SF_{dc}}(\tau)}{\mathrm{SF_{tot}}(\tau)}, \quad (1)$$

where $\mathrm{SF_{ic}}$, $\mathrm{SF_{dc}}$, and $\mathrm{SF_{tot}}$ are the SF based on brightening pairs, fading pairs, and total pairs, respectively. A negative β would imply a gradual rise and rapid fading in the light curve, as expected from the model of accretion disk instabilities (Kawaguchi et al. 1998). While earlier measurements of this β statistic were inconclusive based on various quasar samples (e.g., Giveon et al. 1999; Hawkins 2002; de Vries et al. 2005; Bauer et al. 2009; Chen & Wang 2015), a statistically significant negative β was reported in more recent variability studies based on large quasar samples from the Sloan Digital Sky Survey (SDSS) Stripe 82 (Voevodkin 2011) and the Catalina Real-Time Transient Survey (CRTS) bright quasar sample (Tachibana et al. 2020), with ∼10 yr long light curves.

In the meantime, modeling stochastic quasar variability with Gaussian processes has gained popularity. The Damped Random Walk (DRW) model is a simple stationary, time-symmetric Gaussian process shown to fit the general optical variability of quasars well (e.g., Kelly et al. 2009; MacLeod et al. 2010). Despite its popularity and overall success in fitting quasar light curves, there are concerns about the applicability of the DRW model (e.g., Mushotzky et al. 2011). If true, the reported asymmetry in the SF would also imply deviations of quasar variability from a DRW, or time-symmetric Gaussian processes in general.

However, there is a selection bias in the samples of quasars used for long-term variability studies that could potentially lead to artificial trends misinterpreted as physical. Many recent quasar variability studies are based on spectroscopically confirmed SDSS quasars, with light curves compiled from different photometric surveys later on. The quasar sample defined earlier on is typically flux limited, and contains more fainter (in terms of the mean luminosity, because quasars are variable) quasars scattered above the flux limit than those scattered below, which would eventually scatter down given sufficient time.[4] Therefore, statistically the sample will have more dimmed quasars than brightened ones when observed at later epochs, as confirmed in observations (e.g., Francis 1996; Rumbaugh et al. 2018; Caplar et al. 2020). This asymmetry in quasar brightness changes at later times was interpreted as a selection bias (e.g., Francis 1996) and modeled with simulated light curves (e.g., Rumbaugh et al. 2018; Luo et al. 2020). The same bias should also lead to an asymmetry in the SF, with an overall negative β as defined in Equation (1).

In this work we quantify the effects of this sample bias using simulated data. We describe our simulations and main results in Section 2. We discuss our findings in Section 3 and conclude in Section 4. The light curve analysis is performed in magnitude

[4] In the case of a DRW, the typical turnaround timescale is the damping timescale, which is about hundreds of days in the quasar rest-frame (e.g., MacLeod et al. 2010).

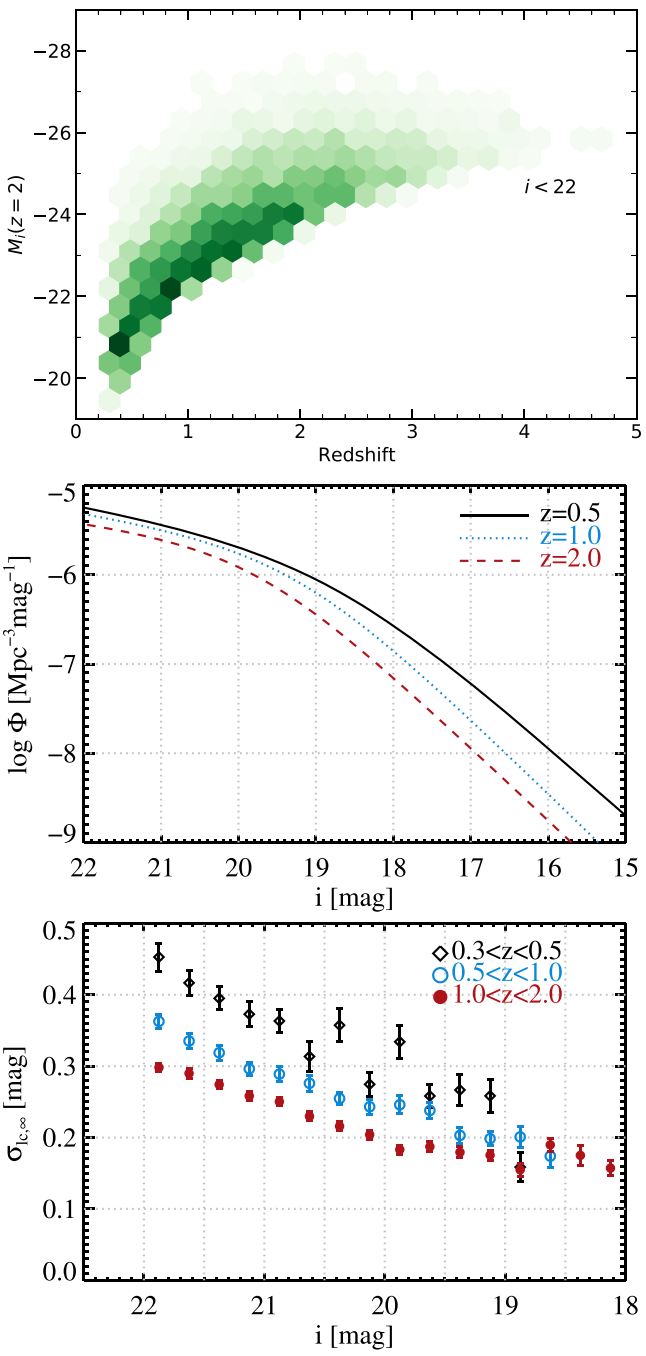

Figure 1. Basic properties of the simulated quasar sample in Section 2.2. Top panel: luminosity (denoted by $M_i(z=2)$, see Richards et al. 2006) and redshift distribution of the simulated quasar sample (higher density regions denoted by darker colors). Middle panel: adopted LF at three redshifts. Bottom panel: sample-median rms of the light curves $\sigma_{\rm lc,\infty} = {\rm SF}_\infty/\sqrt{2}$ in different magnitude-redshift bins.

units following the common practice for optical quasar variability studies.

2. Methods and Results

2.1. A Toy Model

The aforementioned bias is a common feature of flux-limited samples with scatters in the observed quantities, and is a generalized form of the Eddington bias (Eddington 1913). Here we use a toy model to illustrate this bias. The instantaneous (noise-free) magnitude m' given mean magnitude m is assumed to be a Gaussian random variable $G(m, \sigma_{\rm lc})$ with mean value m and rms dispersion $\sigma_{\rm lc}$. The underlying quasar luminosity function (LF) $\Phi(m)$ (in units of space density per mag), is assumed to be a single power-law $\Phi(m) \propto 10^{\gamma m}$, where the slope $\gamma > 0$ (in units of mag^{-1}).

This simple model leads to a constant bias between the instantaneous magnitude and the mean magnitude in the sample (e.g., Shen & Kelly 2010):

$$A \equiv m' - <m> = -\ln(10)\gamma\sigma_{\rm lc}^2. \quad (2)$$

At each instantaneous magnitude m', the number ratio of quasars with $m > m' + \Delta m$ and with $m < m' - \Delta m$, where $\Delta m \geqslant 0$ is a given threshold in magnitude differences, is

$$R = \frac{\int_{m'+\Delta m}^{+\infty} 10^{\gamma m} e^{-\frac{(m-m')^2}{2\sigma_{\rm lc}^2}} dm}{\int_{-\infty}^{m'-\Delta m} 10^{\gamma m} e^{-\frac{(m-m')^2}{2\sigma_{\rm lc}^2}} dm} = \frac{1 - {\rm erf}[(\Delta m + A)/\sqrt{2\sigma_{\rm lc}^2}]}{1 + {\rm erf}[(-\Delta m + A)/\sqrt{2\sigma_{\rm lc}^2}]}, \quad (3)$$

where erf(x) is the Gauss error function.

When the sample with fixed m' is frozen at t_0 and re-observed at late times (or at earlier times), the mean flux will be fainter by $|A|$ magnitude, and there will be an overabundance of dimmed quasars expected from Equation (3). The probability distribution of magnitude will be a Gaussian with mean $m' - A$ and dispersion $\sigma_{\rm lc}$. If the time lapse since sample selection is longer than the characteristic damping timescale, the rms variation $\sigma_{\rm lc} \approx {\rm SF}_\infty/\sqrt{2}$, where ${\rm SF}_\infty$ is the asymptotic structure function on very long timescales. Given a typical bright-end slope of the LF $\gamma = 0.8$ and $\sigma_{\rm lc} = 0.2$, we have $A \sim -0.1$ mag, which is a small effect to measure with a large sample of quasars (Caplar et al. 2020), and an overabundance of dimmed quasars of $N_{\rm dimmed}/N_{\rm brightened} \approx 1.8$, 3.5 for $|\Delta m| = 0$, 0.25. The comparisons above are between the epoch of sample selection and a different epoch. If we move sufficiently far away from the selection epoch (typically a few years, e.g., the damping timescale multiplied by $1+z$), the distribution of observed magnitude will converge to the same Gaussian with mean $m' - A$ and dispersion $\sigma_{\rm lc}$, and the time asymmetry between two different epochs will largely go away.

In practice, the real flux-limited sample covers a range of magnitudes, redshifts, and variability characteristics, and the effects of this sample bias are best studied with simulated data (Section 2.2). Nevertheless, this toy model provides an intuitive understanding of the observed trends.

2.2. Simulated Quasar Sample and Light Curves

We start by generating a large sample of quasars at $0.3 < z < 5$ following the observed optical LF at different redshifts (Hopkins et al. 2007). The lower redshift cut is to reduce the impact of host galaxy light on quasar variability. The mock quasar sample was generated to a limiting magnitude of $i_{\rm mean} = 22$, where $i_{\rm mean}$ is the mean magnitude of the quasar. We chose this limiting magnitude above which the quasar LF is well measured from large spectroscopic surveys (e.g., Richards et al. 2006). The imposed flux limits to define our quasar sample for variability studies will be far from $i = 22$, therefore

missing the $i > 22$ faint quasar population will not affect our results. Figure 1 (top panel) shows the distribution of simulated quasars in the $L - z$ plane. There are in total ~200,000 simulated quasars at $i < 22$, ensuring that we have sufficient statistics when restricting the sample to brighter flux limits.

For each simulated quasar, we assign luminosity and black hole mass following empirical relations derived for SDSS quasars (Richards et al. 2006; Shen et al. 2011). We then use the empirical relations in MacLeod et al. (2010) to assign DRW parameters and generate a stochastic i-band light curve for each quasar with a daily cadence over an observed baseline of 20 yr. The mock light curve varies around the mean i-band magnitude of the quasar.

For each light curve, we compute the rest-frame SF

$$\mathrm{SF}(\tau) = \left[\frac{1}{N(\tau)}\sum_{i<j}(x_i - x_j)^2\right]^{1/2}, \quad (4)$$

where i and j are indices of the time series, $N(\tau)$ is the number of pairs in each rest-frame time τ bin of the SF, and x_i and x_j are the corresponding magnitudes at times t_i and t_j for these pairs. $\mathrm{SF_{ic}}$ and $\mathrm{SF_{dc}}$ are computed using pairs with increasing and decreasing fluxes, respectively; $\mathrm{SF_{tot}}$ uses all pairs. We verify that the ensemble SF is consistent with the DRW prediction, while individual light curves (particularly high-redshift quasars with long observed-frame damping timescales) may deviate from the DRW prediction due to stochasticity over the limited observing baseline.

To define a flux-limited sample constructed at an earlier epoch, we use the first light curve point at t_0. This is a key step to properly mimic the real sample selection. In earlier studies (e.g., Tachibana et al. 2020), while not explicitly stated, we suspect that the mock sample was constructed using the mean magnitude instead of the instantaneous magnitude at the selection epoch. This detail will lead to distinctive outcomes from simulated light curves, as we demonstrate below.

Rumbaugh et al. (2018) and Luo et al. (2020) have shown that when observing a flux-limited quasar sample in a later survey, dimmed quasars will outnumber brightened quasars and this asymmetry increases when the threshold of the magnitude change $|\Delta m|$ increases. While the exact levels of the asymmetry depend on the simulated quasar population (e.g., the shape of the LF)[5] and adopted DRW parameters, we confirm these general trends in Figure 2 using our simulated quasar samples at various flux limits and thresholds in magnitude changes.

While the asymmetry in the numbers of dimmed and brightened quasars is prominent, the mean magnitude change of the whole sample is mild, because most of the time pairs have small differences in magnitude. The mean magnitude differences after 10 yr in the observed frame for our simulated sample of $i_{t_0} < 19$ is ~0.1 mag fainter, roughly matching the observed mean magnitude change in Caplar et al. (2020). This mean magnitude bias is stronger at lower redshifts (at fixed flux limit), because the rms variability amplitude is higher (Figure 1 and Equation (2)), again consistent with the findings in Caplar et al. (2020).

Figure 3 shows the resulting asymmetry in the ensemble SF measurements, using a fiducial simulated quasar sample with

[5] Our adopted LF has a power-law form at the bright end; a steeper drop of the bright-end LF would lead to more severe bias for brighter samples.

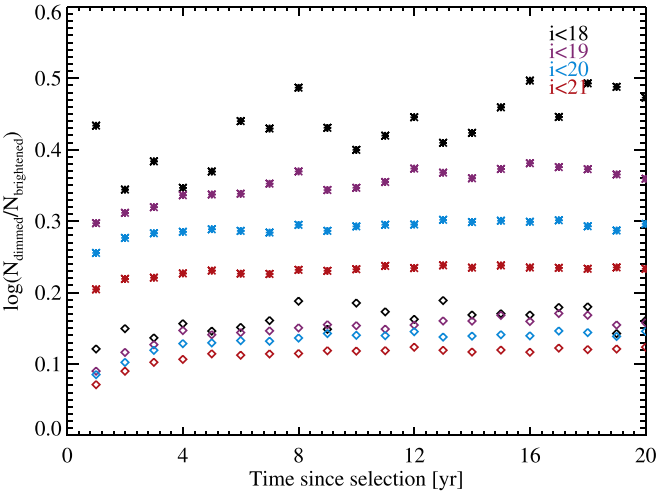

Figure 2. Ratio of the numbers of dimmed and brightened quasars as a function of time. Different colors denote different flux limits in the sample. The diamonds are for a magnitude change threshold of $|\Delta m| = 0$ and the asterisks are for a magnitude change threshold of $|\Delta m| = 0.25$.

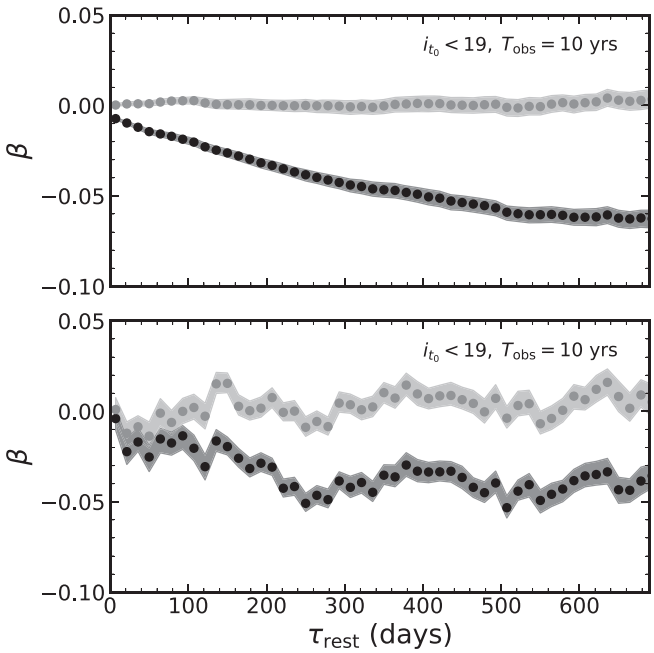

Figure 3. Time asymmetry in the SF for a simulated quasar sample of $i_{t_0} < 19$ over a 10 yr baseline in the observed frame. Top panel: results from the ideal light curves. Bottom panel: results from downgraded light curves that mimic the CRTS light curves. In each panel, the black dots and shaded band are the measured SF asymmetry $\beta(\tau)$ and 1σ uncertainties for the flux-limited sample, and the gray dots and shaded band are the results for a comparison sample with $i_{\mathrm{mean}} < 19$; the latter is not a flux-limited sample at selection. Uncertainties on β are estimated from bootstrap resampling.

$i_{t_0} < 19$ and a 10 yr observational baseline that starts at the selection epoch t_0. This flux-limited mock sample and light curve duration roughly match those of the bright CRTS quasars studied in Tachibana et al. (2020). Because the CRTS sample is a bright quasar sample ($V < 18$), most of the quasars come from SDSS-I/II legacy surveys based on SDSS targeting photometry a few years earlier than the bulk of the CRTS light curves.

The top panel of Figure 3 shows the results based on the noise-free, daily-sampled mock light curves, and the bottom panel shows the results based on downgraded light curves to

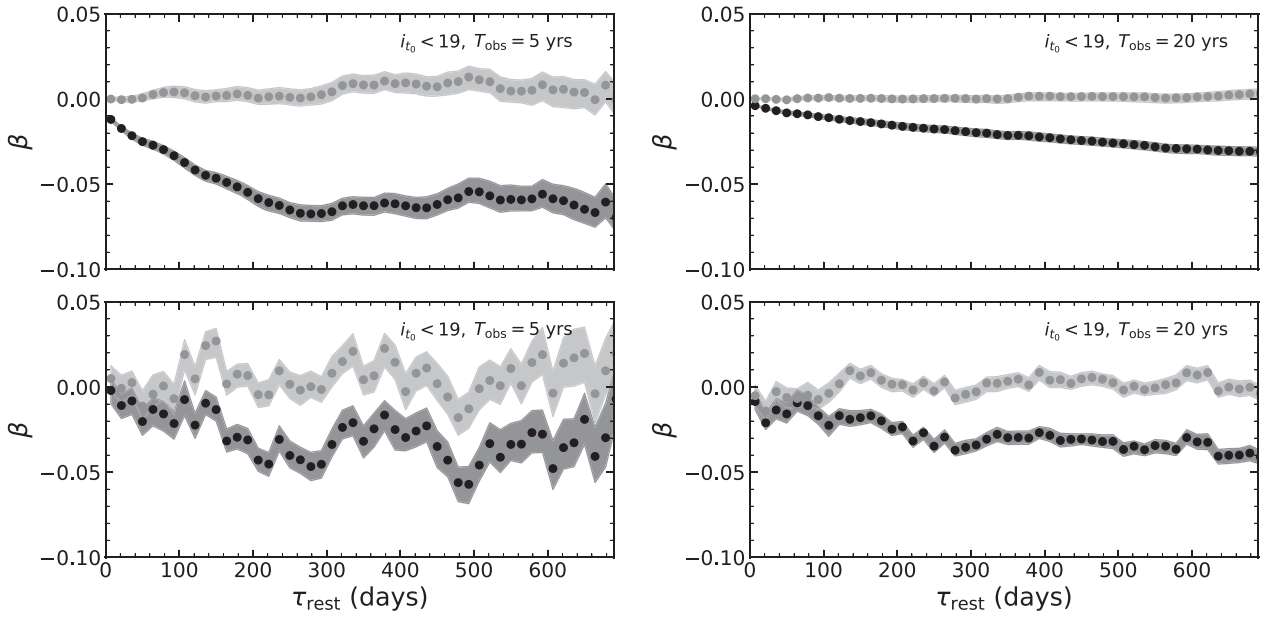

Figure 4. Similar to Figure 3, but for different light curve durations. SF measurements are noisier for shorter durations due to fewer pairs from the light curve.

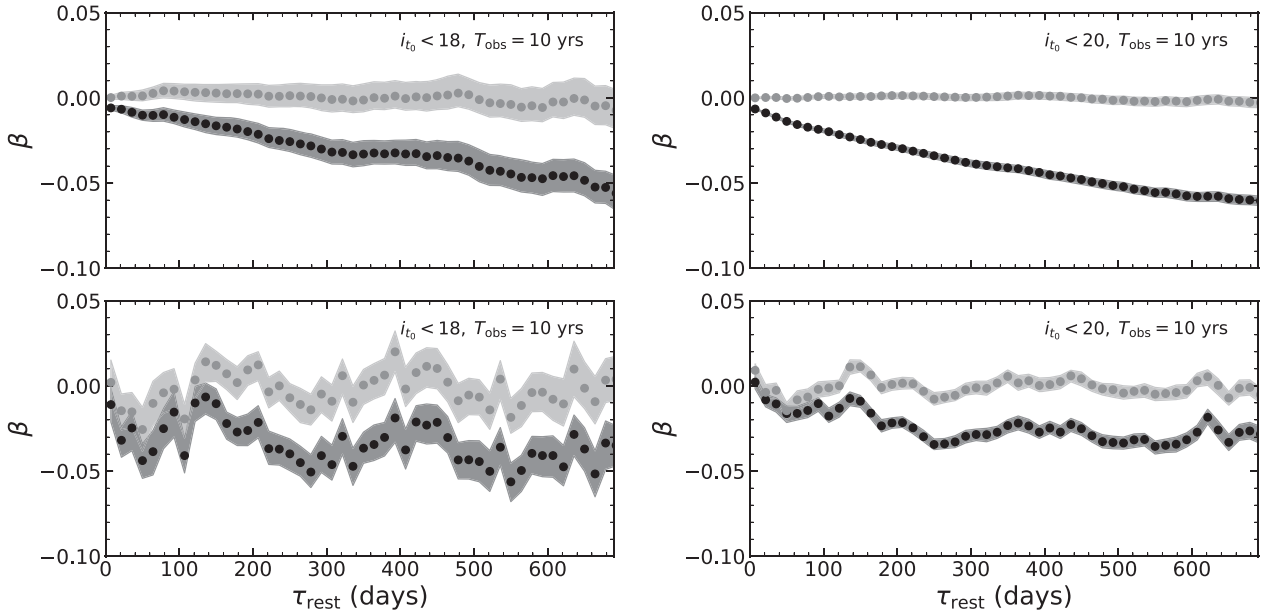

Figure 5. Similar to Figure 3, but for different flux limits at the selection. SF measurements are noisier for brighter limits due to fewer quasars in the sample.

mimic the cadence, seasonal gaps, and magnitude uncertainties in the CRTS sample. The results from downgraded light curves are noisier than those from the ideal light curves, but still reproduce the overall trend of β. As expected, the flux-limited sample defined at t_0 results in an asymmetric SF such that $\mathrm{SF_{ic}}$ is systematically smaller at the few percent level than $\mathrm{SF_{dc}}$, similar to the observed trend in the CRTS sample. For comparison, the gray lines in Figure 3 show the results of a control sample selected with $i_{\rm mean} < 19$, where β is consistent with zero as expected. Uncertainties are estimated based on bootstrap resampling.

In our fiducial calculations of β, we have used the mean SFs over the sample. Using the median SFs, or the median/mean of the β distribution from individual quasars produces similar results.

3. Discussion

Figures 4 and 5 show the resulting β for different flux limits and light curve lengths. The time asymmetry of the SF is insensitive to the flux limit, mainly due to the combined effects of LF steepening and decreasing variability toward the bright end (see Equation (2) and Figure 1). On the other hand, this bias is somewhat alleviated for longer baselines. The latter trend is straightforward to understand (Section 2.1). Pairs of epochs contributing to the SF that are both far away from the selection epoch do not retain the memory of the time

asymmetry. The longer the length of the light curve, the more dilution from these epochs to reduce the overall time asymmetry caused by pairs that include the selection epoch. In addition, the decorrelation timescale (i.e., the DRW damping timescale) will also affect the exact level of this asymmetry in the ensemble SF. Our adopted DRW damping timescales from MacLeod et al. (2010) are reasonable, but some quasars may have even longer damping timescales to worsen this sample bias.

Overall, our simulations predict negative β over multi-year baselines roughly starting from the selection epoch. Tachibana et al. (2020) also found positive β for rest-frame SF time $\tau \lesssim 100$ days (peaking around $\sim$40 days). The SF measurements are more affected by magnitude uncertainties at shorter timescales due to the smaller SF amplitude. In addition, some of these short-timescale pairs could come from CRTS photometry prior to the SDSS selection that captured more rising segments of the light curve. Nevertheless, it is possible that this positive β at $\tau \lesssim 100$ days is real, and may reflect underlying driving mechanisms of the short-time variability (e.g., Kawaguchi et al. 1998; Tachibana et al. 2020).

This sample bias also explains negative and zero β values reported in other studies of quasar light curves. If the SFs are computed using historic photometric data for a flux-limited sample defined at a later epoch, then this bias will lead to on average positive β values, as reported in de Vries et al. (2005) with historic imaging data for SDSS quasars (the photometry at the SDSS epoch was also used in the SF calculation). However, if the light curves are far away from the sample selection epoch, or if the sample is not a flux-limited sample or there is no clearly defined selection epoch, then there should be no time asymmetry in the ensemble SF ($\beta \approx 0$, e.g., Hawkins 2002; Chen & Wang 2015). We have confirmed these predicted trends of β with our simulated data.

4. Conclusions

With ever-increasing sample statistics and extended baselines for variability studies, it has now become feasible to explore subtle ensemble variability characteristics of quasars. It is notoriously difficult to interpret light curves with physical models to understand the nature of quasar variability, given the broad range of stochastic processes that can describe the observed time series (e.g., Scargle 2020). Salient ideas have been proposed that use simple statistics of the time series to explore specific aspects of quasar variability, e.g., the time asymmetry in the ensemble SF (e.g., Kawaguchi et al. 1998), the rms-flux relation (Uttley & McHardy 2001), and characteristic timescales in the variability power spectrum (e.g., McHardy et al. 2006; Burke et al. 2021). The hope is that with the correct interpretation of these statistics, one can infer the physical mechanisms of quasar variability.

In this work we have highlighted a sample bias introduced at the time of sample selection, in light of recent reports of time asymmetry in optical quasar variability observed over extended periods. With simulated quasars that follow the observed luminosity-redshift distribution, and simulated time-symmetric light curves based on the DRW model, we demonstrated the effects of this bias for flux-limited samples selected at an earlier epoch and re-observed at later times with a multi-year baseline:

1. there will be more dimmed than brightened quasars observed at later times, and the sample mean flux will fade by a small amount ($\sim$0.1 mag);
2. there is an asymmetry in the SF measured from increasing-flux pairs and decreasing-flux pairs at the few percent level.

Both predictions based on simulated data are similar to observed trends (Voevodkin 2011; Caplar et al. 2020; Tachibana et al. 2020). The selection of a flux-limited quasar sample at certain epoch inevitably incorporates an asymmetry in variability, because there are more temporarily brightened quasars above the flux limit than those falling below. This Eddington-like bias is common in statistical studies of survey samples. Depending on what light curves are used (i.e., before or after the sample selection epoch, and the length of the light curves), the β statistic defined in Equation (1) can either be positive, negative, or zero (Section 3).

While our results do not necessarily imply that the DRW model is correct, they provide a cautionary note on recent claims that there is a time asymmetry in quasar light curves based on bright, (approximately) flux-limited samples. The manifestation of this bias, in terms of the mean magnitude changes and the asymmetry in the SF, is generally small and only detectable with large statistical quasar samples as those studied in, e.g., Caplar et al. (2020) and Tachibana et al. (2020).

To mitigate this bias, one could potentially do one of the following: (1) use the later-epoch photometry to select a second flux-limited sample (with the same flux limit) that will recover those missed in the initial sample, and average the results from the two flux-limited samples; (2) carefully adjust the initial sample to include equal numbers of brightened and faded quasars in each $|\Delta\mathrm{mag}|$ bin; or (3) use portions of light curves that are at least a few years away from the sample selection epoch. On the other hand, if the quasar LF can be accurately measured, the observed apparent asymmetry in ensemble quasar light curves may be used to provide independent constraints on quasar variability, e.g., the luminosity dependences of the variability amplitude and damping (decorrelation) timescale.

We thank the referee for useful comments that improved the presentation of this work. Y.S. was supported by NSF grant AST-2009947. C.J.B. acknowledges support from the Illinois Graduate Survey Science Fellowship.

ORCID iDs

Yue Shen https://orcid.org/0000-0003-1659-7035
Colin J. Burke https://orcid.org/0000-0001-9947-6911

References

Bauer, A., Baltay, C., Coppi, P., et al. 2009, ApJ, 696, 1241
Burke, C. J., Shen, Y., Blaes, O., et al. 2021, Sci, 373, 789
Caplar, N., Lilly, S. J., & Trakhtenbrot, B. 2017, ApJ, 834, 111
Caplar, N., Pena, T., Johnson, S. D., & Greene, J. E. 2020, ApJL, 889, L29
Chen, X.-Y., & Wang, J.-X. 2015, ApJ, 805, 80
de Vries, W. H., Becker, R. H., White, R. L., & Loomis, C. 2005, AJ, 129, 615
Eddington, A. S. 1913, MNRAS, 73, 359
Francis, P. J. 1996, PASA, 13, 212
Giveon, U., Maoz, D., Kaspi, S., Netzer, H., & Smith, P. S. 1999, MNRAS, 306, 637
Hawkins, M. R. S. 2002, MNRAS, 329, 76
Hopkins, P. F., Richards, G. T., & Hernquist, L. 2007, ApJ, 654, 731

Kawaguchi, T., Mineshige, S., Umemura, M., & Turner, E. L. 1998, ApJ, 504, 671
Kelly, B. C., Bechtold, J., & Siemiginowska, A. 2009, ApJ, 698, 895
Luo, Y., Shen, Y., & Yang, Q. 2020, MNRAS, 494, 3686
MacLeod, C. L., Ivezić, Ž., Kochanek, C. S., et al. 2010, ApJ, 721, 1014
McHardy, I. M., Koerding, E., Knigge, C., Uttley, P., & Fender, R. P. 2006, Natur, 444, 730
Mushotzky, R. F., Edelson, R., Baumgartner, W., & Gandhi, P. 2011, ApJL, 743, L12
Richards, G. T., Strauss, M. A., Fan, X., et al. 2006, AJ, 131, 2766
Rumbaugh, N., Shen, Y., Morganson, E., et al. 2018, ApJ, 854, 160
Scargle, J. D. 2020, ApJ, 895, 90
Shen, Y., & Kelly, B. C. 2010, ApJ, 713, 41
Shen, Y., Richards, G. T., Strauss, M. A., et al. 2011, ApJS, 194, 45
Tachibana, Y., Graham, M. J., Kawai, N., et al. 2020, ApJ, 903, 54
Uttley, P., & McHardy, I. M. 2001, MNRAS, 323, L26
Vanden Berk, D. E., Wilhite, B. C., Kron, R. G., et al. 2004, ApJ, 601, 692
Voevodkin, A. 2011, arXiv:1107.4244